J. Automation & Systems Engineering 12-3 (2018): 12-25

Regular paper

Implementation of Control Strategy Based on SVM for Open-End Winding Induction Motor with short circuit fault between turns in Stator Windings

Saad Khadar [1] and A. Kouzou [1]

[1] LAADI Laboratory, Faculty of Technology Zian Achour University, 17000 Djelfa, Algeria

(saad.khadarpc1@gmail.com, kouzouabdellah@ieee.org)

Abstract*-Open-end winding induction motors have a lot of advantages in comparison to conventional induction motors due to their reliability. However, their sudden failures can result in significant plant downtime and great economical losses. This suggests the development of control strategies for improving reliability. Consequently, this paper proposes a mathematical model by which the behaviour of Open-end winding induction motor with a short circuit fault between turns can be analyzed. In addition, a new nonlinear backstepping control based on space vector modulation, taking into consideration the stator faults is used to ensure the continuous operation of the motor before the required maintenance can be done. The numerical validation results demonstrate that the proposed control strategy have presented good performances of motor in healthy and faulty conditions.

Keywords: Open-End Winding, Induction Motor (IM), Backstepping Control, Space Vector Modulation (SVM), Electromagnetic Coupling, Short Circuit Fault Between Turns.

1. INTRODUCTION

In recent years, the open-end winding induction machine topology fed by dual-inverter possesses some advantages over the traditional single-sided supply configurations. The main features of an open-winding induction machine can be summarized as [1]. These motors are placed in varying environments and conditions can affect its reliability. Commonly the damage mechanism of machine can be categorized according to the main components such as the stator, rotor, and bearings. According to failure surveys [2, 3] concluded that bearing related failures are 40% of the motor failures, stator winding failures are 38%, rotor related failures are 10% and 12% affect other part of machine are treated as mixed failures. Faults in the motor stator winding represent a significant percentage of motor failures. Also, these surveys indicate that the majority of stator circuit failures result from breakdown of the short-circuits between turns [4]. When a short-circuits between turns fault occurs, extremely high current flows through the shorted turns of the stator winding, which produces excessive heat in the surrounding insulation [5]. This further degrades the insulation and finally results into line-to-line, phase-to-ground and multi-phase line-to ground [6, 7], which decreases the motor efficiency and accelerates motor degradation [8], if left undetected or untreated. So, early faults detection and diagnosis in the machine is an important task to ensure reliability and reduce repairing cost. Recent years, many condition monitoring techniques have been presented for different types of fault modeling and detection. For example in [9,10] axial leakage flux monitoring was used as a method for detecting the occurrence of short-circuits between turns by means of a large

coil fixed concentri-cally around of the shaft of the motor. In [11] and [12], proposed a method to detect stator faults using the structural parameters of knowledge model. Indeed, the method of stator faults will be based on the model used [11,12].

Another topic of great importance is the machine modeling under fault conditions. Instead of a binary decision on fault detection. Modeling of machine with fault conditions is a key to predicting its behavior [13]. The analysis of stator faults can be made by different models. Several modeling and simulation studies have been published, related to the analysis of the stator faults of synchronous and asynchronous motors [14]–[17]. In fact, a more precise modelling of the machine is necessary for an accurate analysis of the machine behavior in both healthy and faulty cases, it is necessary to consider its electromagnetic behaviour. The aim of this paper is to develop a mathematical model of an open-end winding induction motor under short circuit fault between turns in the stator winding. This model is based on the theory of electromagnetic coupling of electrical circuits.

In general, when a short-circuits between turns fault occurs, a motor failure can result in the shutdown of a generating unit or production line and this suggests the development of control strategies for improving reliability. Based on the above discussion, the research effort presented in this paper focuses on the nonlinear Backstepping control based on space vector modulation to improve the performance of open-end winding induction motor operating under short circuit fault between turns in the stator winding. This control strategy is capable on continue operation of the motor under healthy as well as faulty conditions. Therefore, the main goal of the proposed control strategy is to prevent unscheduled downtime of these machines.

The remainder of the paper is organized as follows; Section 2 introduces the modeling of an open-end winding induction motor with stator faults. Then, the Backstepping control using space vector modulation is explained in details in section 3. Finally, simulation results and conclusion are given in the last Section.

2. MODELING OF INDUCTION MOTOR WITH STATOR FAULTS

The stator faults are very common faults in electrical machines while operating in industries, the short circuit fault between turns represents the origin and cause of other faults. The persistence of the latter will promotes the emergence of other cases of short circuit [18]. A open-end winding induction motor with stator winding turn fault at phase (A) is shown in Figure. 1, where N_{cc} represents the number of turns in short circuit in phase (A) and N_s is the number of turns in the healthy state.

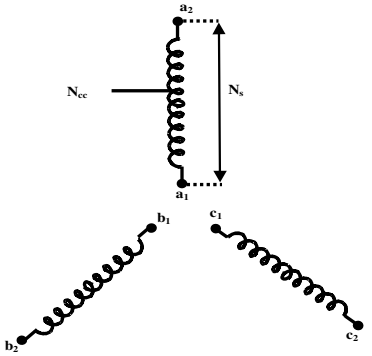

Figure 1 Stator winding scheme with a short-circuits fault between turns

To modelling the faults a short-circuits fault between turns, we can apply another method for modelling of the IM, taking into account the changing parameters such as; the matrix of

stator resistance and the matrix of the stator inductances and mutual inductance stator-rotor are variables [19]. Here are the following short-circuit coefficients:

Short-circuit coefficient relative to the A- phase: $k_{sa} = \frac{N_{cc}}{N_s}$

Short-circuit coefficient relative to the B-phase: $k_{sb} = \frac{N_{cc}}{N_s}$

Short-circuit coefficient relative to the C- phase: $k_{sc} = \frac{N_{cc}}{N_s}$

We definite the total number of turns in all three stator phases :

$$\begin{cases} N_1 = N_s - N_{cc} = (1-k_{sa})N_s = h_{sa}N_s \\ N_2 = N_s - N_{cc} = (1-k_{sb})N_s = h_{sb}N_s \\ N_3 = N_s - N_{cc} = (1-k_{sc})N_s = h_{sc}N_s \end{cases} \quad (1)$$

The matrixes $[L_S],[M_{SS}],[M_{SR}],[M_{RS}]$ and $[R_S]$ depend on the three ratio h_{sa}, h_{sb}, h_{sc} can be written as:

$$[R_S] = R_s \begin{pmatrix} h_{sa} & 0 & 0 \\ 0 & h_{sb} & 0 \\ 0 & 0 & h_{sc} \end{pmatrix}, \quad [L_S] = L_s \begin{pmatrix} h_{sa}^{\,2} & 0 & 0 \\ 0 & h_{sb}^{\,2} & 0 \\ 0 & 0 & h_{sc}^{\,2} \end{pmatrix}$$

$$[M_{SS}] = M_{ss} \begin{pmatrix} h_{sa}^{\,2} & -\frac{h_{sa}h_{sb}}{2} & -\frac{h_{sa}h_{sc}}{2} \\ -\frac{h_{sa}h_{sb}}{2} & h_{sb}^{\,2} & -\frac{h_{sc}h_{sb}}{2} \\ -\frac{h_{sa}h_{sc}}{2} & -\frac{h_{sc}h_{sb}}{2} & h_{sc}^{\,2} \end{pmatrix}, \quad [M_{SR}] = M_{sr} \begin{pmatrix} h_{sa}\cos\theta & h_{sa}\cos(\theta+\frac{2\pi}{3}) & h_{sa}\cos(\theta-\frac{2\pi}{3}) \\ h_{sb}\cos(\theta-\frac{2\pi}{3}) & h_{sb}\cos\theta & h_{sb}\cos(\theta+\frac{2\pi}{3}) \\ h_{sc}\cos(\theta+\frac{2\pi}{3}) & h_{sc}\cos(\theta-\frac{2\pi}{3}) & h_{sc}\cos\theta \end{pmatrix}$$

With: $[M_{SR}] = [M_{RS}]^T$

When the motor is running, the coefficient matrix is not constant; they vary depending on the angle, angular position between the rotor and the stator. This makes the model phase equivalent hardly usable both in control and the monitoring, in the approach that follows a mathematical transformation is applied to the equations of the previous model in order to make the entire calculable online. Using this transformation, all variables rotor can be changed into new variables with the same pulsation that the variables stator. Thus, all parameters of the model will be independent of the angular position, the conversion is given by the following matrix [19]:

$$[T] = \begin{pmatrix} \cos(\theta)+\frac{1}{2} & \cos(\theta+\frac{2\pi}{3})+\frac{1}{2} & \cos(\theta-\frac{2\pi}{3})+\frac{1}{2} \\ \cos(\theta-\frac{2\pi}{3})+\frac{1}{2} & \cos\theta+\frac{1}{2} & \cos(\theta+\frac{2\pi}{3})+\frac{1}{2} \\ \cos(\theta+\frac{2\pi}{3})+\frac{1}{2} & \cos(\theta-\frac{2\pi}{3})+\frac{1}{2} & \cos(\theta)+\frac{1}{2} \end{pmatrix} \quad (2)$$

Using the same steps as those of the transformed PARK, we get the new three phase model which represent the global model of the induction motor in the presence of stator faults can be introduced as follows:

$$\begin{cases} \dfrac{d\varphi_{ra}}{dt} = \lambda\left(h_{sa} i_{sa} - \dfrac{h_{sb}}{2} i_{sb} - \dfrac{h_{sc}}{2} i_{sc} \right) - \dfrac{R_r.A}{C}\varphi_{ra} - \left(\dfrac{R_r.B}{C} + \dfrac{\sqrt{3}}{3}\omega \right)\varphi_{rb} - \left(\dfrac{R_r.B}{C} - \dfrac{\sqrt{3}}{3}\omega \right)\varphi_{rc} \\ \dfrac{d\varphi_{rb}}{dt} = \lambda\left(-\dfrac{h_{sa}}{2} i_{sa} + h_{sb} i_{sb} - \dfrac{h_{sc}}{2} i_{sc} \right) - \left(\dfrac{R_r.B}{C} - \dfrac{\sqrt{3}}{3}\omega \right)\varphi_{ra} - \dfrac{R_r.A}{C}\varphi_{rb} - \left(\dfrac{R_r.B}{C} + \dfrac{\sqrt{3}}{3}\omega \right)\varphi_{rc} \\ \dfrac{d\varphi_{rc}}{dt} = \lambda\left(-\dfrac{h_{sa}}{2} i_{sa} - \dfrac{h_{sb}}{2} i_{sb} + h_{sc} i_{sc} \right) - \left(\dfrac{R_r.B}{C} + \dfrac{\sqrt{3}}{3}\omega \right)\varphi_{ra} - \left(\dfrac{R_r.B}{C} - \dfrac{\sqrt{3}}{3}\omega \right)\varphi_{rb} - \dfrac{R_r.A}{C}\varphi_{rc} \end{cases} \quad (3)$$

The stator currents expressed as:

$$\begin{cases} \dfrac{di_{sa}}{dt} = V_{SA} + K_{A1} i_{sa} + K_{A2} i_{sb} + K_{A1} i_{sc} + k.h_{sa} h_{sb}^2 h_{sc}^2 \left[G\varphi_{ra} + \left(\dfrac{\sqrt{3}}{2}\omega - \dfrac{G}{2} \right)\varphi_{rb} - \left(\dfrac{\sqrt{3}}{2}\omega + \dfrac{G}{2} \right)\varphi_{rc} \right] \\ \dfrac{di_{sb}}{dt} = V_{SB} + K_{B1} i_{sa} + K_{B2} i_{sb} + K_{B1} i_{sc} + k.h_{sa} h_{sb}^2 h_{sc}^2 \left[-\left(\dfrac{\sqrt{3}}{2}\omega + \dfrac{G}{2} \right)\varphi_{ra} + G\varphi_{rb} + \left(\dfrac{\sqrt{3}}{2}\omega - \dfrac{G}{2} \right)\varphi_{rc} \right] \\ \dfrac{di_{sc}}{dt} = V_{SC} + K_{C1} i_{sa} + K_{C2} i_{sb} + K_{C1} i_{sc} + k.h_{sa} h_{sb}^2 h_{sc}^2 \left[\left(\dfrac{\sqrt{3}}{2}\omega - \dfrac{G}{2} \right)\varphi_{ra} - \left(\dfrac{\sqrt{3}}{2}\omega + \dfrac{G}{2} \right)\varphi_{rb} + G\varphi_{rc} \right] \end{cases} \quad (4)$$

With:

$$\begin{aligned} V_{SA} &= d_1 h_{sb}^2 h_{sc}^2 u_{sa} + d_2 h_{sa} h_{sb} h_{sc}^2 u_{sb} + d_2 h_{sa} h_{sb}^2 h_{sc} u_{sc} \\ V_{SB} &= d_2 h_{sa} h_{sb} h_{sc}^2 u_{sa} + d_1 h_{sa}^2 h_{sc}^2 u_{sb} + d_2 h_{sc} h_{sb} h_{sa}^2 u_{sc} \\ V_{SC} &= d_2 h_{sa} h_{sb}^2 h_{sc} u_{sa} + d_2 h_{sc} h_{sb} h_{sa}^2 u_{sb} + d_1 h_{sa}^2 h_{sb}^2 u_{sc} \end{aligned} \quad (5)$$

The setting are:

$$\begin{cases} A = (M_{rr} + L_r)^2 - \dfrac{M_{rr}^2}{4}, B = \dfrac{M_r L_r}{2} + \dfrac{3M_r^2}{4}, C = L_r^3 + 3L_r^2 M_{rr} + \dfrac{9M_{rr}^2 L_r}{4}, G = \dfrac{R_r (A - B)}{C} \\ d_1 = (z + L_r)^2 - \dfrac{z^2}{4}, d_2 = \dfrac{z(z + L_r)}{2} + \dfrac{z^2}{4}, z = M_{SR} - \dfrac{3M_{rr}^2 (A - B)}{2C}, \lambda = \dfrac{M_{SR} R_r (A - B)}{C} \end{cases}$$

The expression for electromagnetic torque developed in the machine are given by the following relation:

$$T_e = \frac{n_p M_{sr}}{L_r}\left[\left(i_{sb}\varphi_{rc} - i_{sc}\varphi_{rb} \right) - \left(i_{sa}\varphi_{rc} - i_{sc}\varphi_{ra} \right) + \left(i_{sa}\varphi_{ra} - i_{sb}\varphi_{rb} \right) \right] \quad (6)$$

Where symbols: R_s, R_r, M_{sr}, L_s, L_r and n_p are stator resistance, rotor resistance, mutual cyclic inductance between stator and rotor, stator cyclic inductance, rotor cyclic inductance and number of pole pairs, respectively, J is the moment of inertia.

The proposed dual three-phase voltage source inverter feeding an open-end winding of the three-phase induction motor is shown in Figure. 2. The dual inverter are identified with indices 1 and 2, where the inverter 1 is connected to stator winding terminal of a_1, b_1 and c_1,

while the inverter 2 is connected to stator winding terminal of a_2, b_2 and c_2, N_1 and N_2 are assumed virtual neutral points of dual inverter. The phase voltages of the dual inverters can be obtained as:

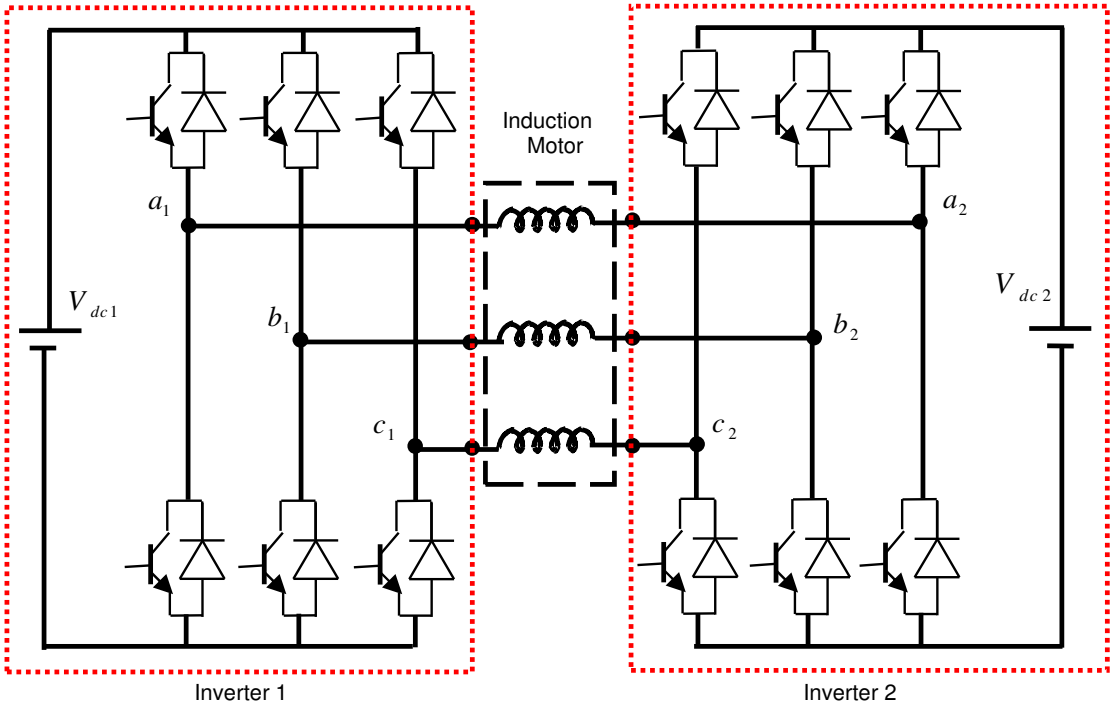

Figure 2 Open-end winding induction motor supplied by dual two-level inverter.

$$\begin{aligned} u_{sa} &= u_{A1N1} - u_{A2N2} \\ u_{sb} &= u_{B1N1} - u_{B2N2} \\ u_{sc} &= u_{C1N1} - u_{C2N2} \end{aligned} \tag{7}$$

Where: u_{A1N1}, u_{B1N1}, u_{C1N1} and u_{A2N2}, u_{B2N2}, u_{C2N2} are the pole voltages of inverter 1 and inverter 2, respectively and u_{sa}, u_{sb}, u_{sc} are the three phase voltages across the phase winding of induction motor. The output voltage space vectors generated by the two inverters expressed in the stationary reference can be written as:

$$\begin{cases} u_{s\alpha 1} + j u_{s\beta 1} = \dfrac{2}{3}(u_{A1N1} + a u_{B1N1} + a^2 u_{C1N1}) \\ u_{s\alpha 2} + j u_{s\beta 2} = \dfrac{2}{3}(u_{A2N2} + a u_{B2N2} + a^2 u_{C2N2}) \end{cases} \tag{8}$$

Where $i=1, 2;$ $\quad a = e^{(i\,2\pi/3)}$

The two-level inverter can generate up to 2^3=8 three dimensional voltage space vectors can be divided into 6 active vectors and two zero vectors. Figure. a3 shows the possible output voltage vectors of the individual inverters. On combination of dual two-level inverter, resulting in a total of switching states 2^3*2^3 = 64 and 19 different space voltage vectors. These vectors can be represented by three hexagons with a center as S; ABCDEF, HJLNPR and GIKMOQ in coordinate system α-β as shown in Figure.b3.

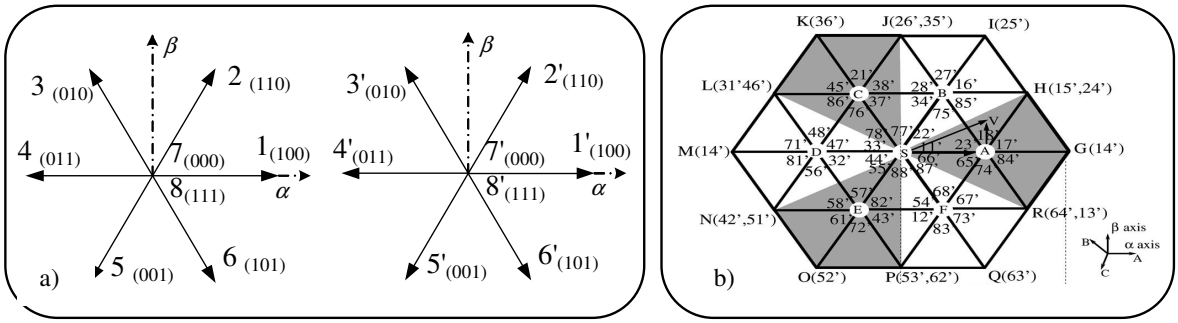

Figure 3 The voltage space vectors for individual inverters and dual inverters in α-β frame.

3. BACKSTEPPING CONTROL BASED ON SPACE VECTOR MODULATION

This work relates to the study of Backstepping control based on SVM of induction motor with open-end winding supplied by dual-inverter. The block diagram of two space vector modulators: SVM_1 and SVM_2 for dual inverter scheme is represented in Figure. 4. In the control scheme, the value of the reference $u_{s\alpha\beta 1}$ and $u_{s\alpha\beta 2}$ are given by the equation (8).

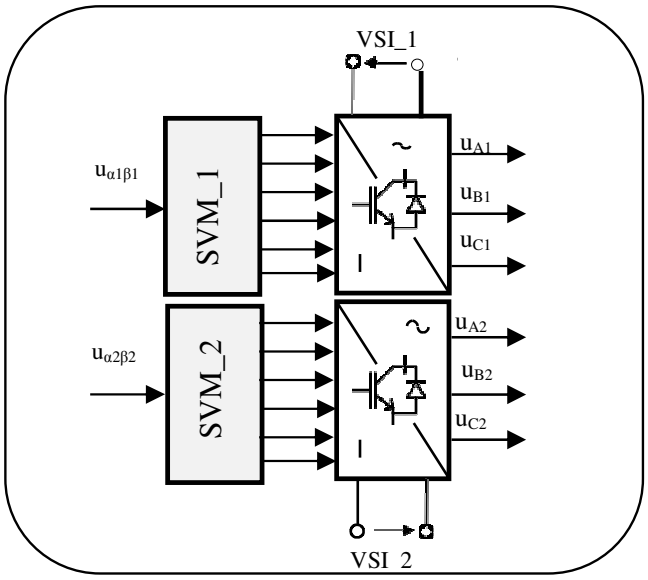

Figure 4 The block diagram of the two space vector modulators.

According to the SVM technique, there would be two sets of phase switching times, for the first inverter 1 and the second inverter 2. For example in sector I, the switching waveforms can be shown in Figure. a5. Within a sampling time period T, the active time for voltage vectors 13' and 24' is T_1 and T_2, respectively, and the residual time T_0 for voltage vectors zero, 77' and 88'. From Figure. 5, within the dead time for the voltage vector of state 13', the switching state of the first inverter 1 are (1 0 0 0 1 1) for (S_{A1}, S_{B1}, S_{C1}, $S_{A1'}$, $S_{B1'}$, $S_{C1'}$) and (0 1 0 1 0 1) for (S_{A2}, S_{B2}, S_{C2}, $S_{A2'}$, $S_{B2'}$, $S_{C2'}$) are the switching state of the second inverter2. For leg A1, the two IGBTs are switched off, and so the freewheeling current through the bottom diode is the only path for the positive winding current, and as to leg A2, the bottom IGBT is turned on for conducting the phase current. Therefore, the two ends of phase a winding are connected to the ground, and then phase a voltage is zero. In other words, for the voltage vector of state 24' , the 3-phase voltages are U_d, 0 and 0, respectively, and for the voltage vector of state 88', all the 3-phase voltages are zero. Figure. b5. shows the vector plane HJLNPR and the SVM waveforms in each sector. In the vector plane, hexagon HJLNPR can be divided into 6 sectors.

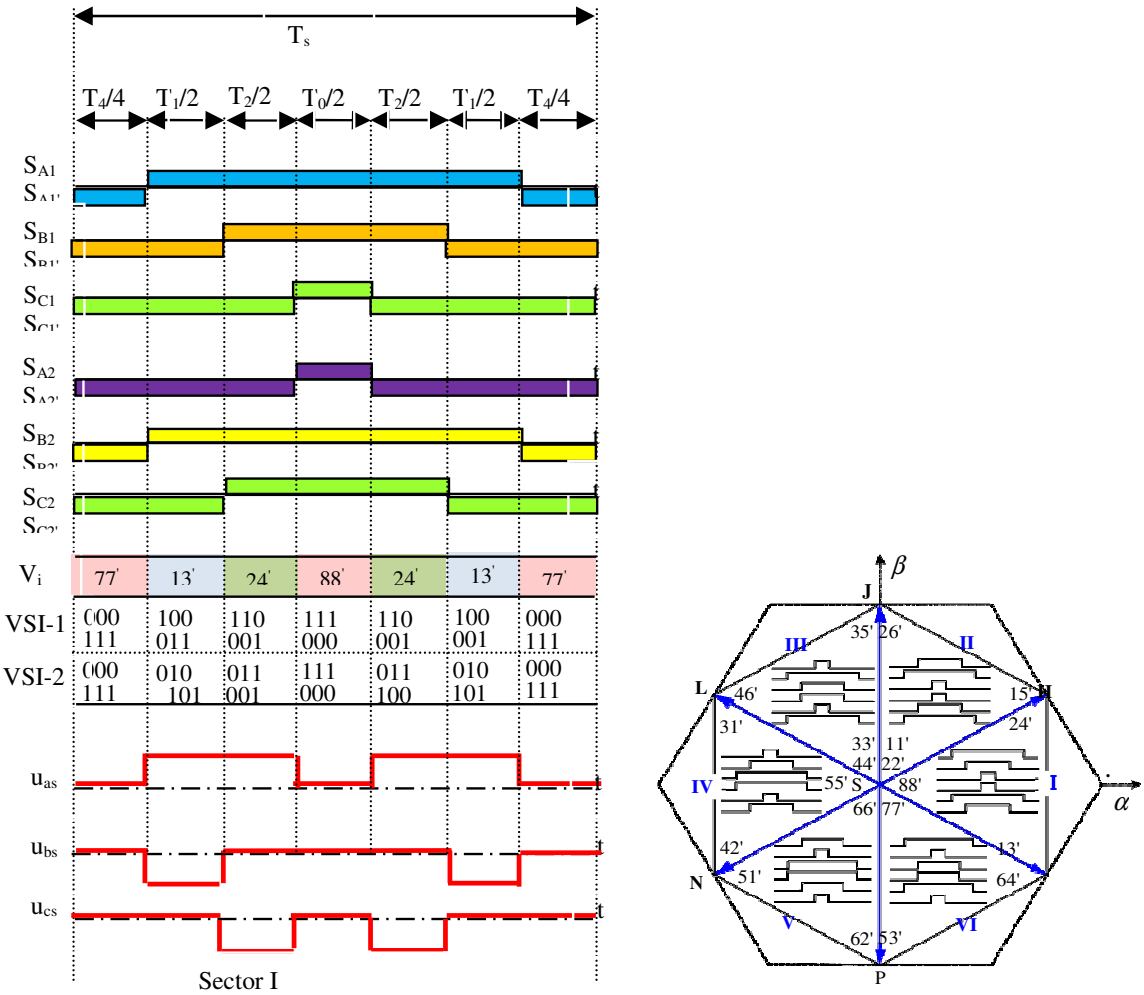

Figure 5 The waveforms of the three phase voltages and the switching states.

The method for Backstepping control of the induction motor is elaborately explained in [20-22] to eliminate conventional PI regulators in vector control. Objective is to force the rotational speed and the rotor flux to follow their references. We use d-q rotating reference frame synchronously with the rotor flux vector $\left[\varphi_{dr}=\varphi_r,\varphi_{qr}=0\right]$. The first step is defined error of the speed and flux as follows:

$$\begin{cases} e_{\omega}=\omega_{ref}-\omega \\ e_{\Psi}=\varphi_{ref}-\varphi_{rd} \\ \dot{e}_{\omega}=\dot{\omega}_{ref}-\dot{\omega} \\ \dot{e}_{\varphi}=\dot{\varphi}_{ref}-\dot{\varphi}_{rd} \end{cases} \tag{9}$$

The Lyapunov function (V_1) associated with the error is chosen as follows:

$$V_1=\frac{1}{2}\left(e_{\varphi}^2+e_{\omega}^2\right) \tag{10}$$

The derivative of V_1 it results in the following expression:

$$\dot{V_1} = \left(-K_\omega e_\omega^2 - K_\varphi e_\varphi^2\right) + e_\omega \left(K_\omega \dot{e_\omega} + \dot{\omega}_{ref} - \eta \varphi_{rd} i_{sq} + \frac{\omega F}{J} + \frac{T_L}{J} \right) + e_\varphi \left(K_\varphi \dot{e_\varphi} + \dot{\varphi}_{ref} + \varphi_{rd} \frac{1}{T_r} - \frac{M_{sr}}{T_r} i_{sd} \right) \quad (11)$$

With: K_φ and K_ω are positive constant. We consider i_{sdref} and i_{sqref} as virtual commands of our first subsystem, and with a suitable choice of these we will render V_1 negative and stabilize the subsystem. From where we draw:

$$\begin{cases} i_{sdref} = \dfrac{T_r}{M_{sr}} \left(K_\varphi e_\varphi + \dot{\varphi}_{rref} + \dfrac{\varphi_{rd}}{T_r} \right) \\ i_{sqref} = \dfrac{1}{\eta \varphi_{rd}} \left(\dot{\omega}_{ref} + K_\omega e_\omega + \dfrac{F\omega}{J} + \dfrac{T_L}{J} \right) \end{cases} \quad (12)$$

Therefore, the derivative of V_1 becomes such as:

$$\dot{V}_1 = \left(-K_\varphi . e_\varphi^2 - K_\omega . e_\omega^2\right) \prec 0 \quad (13)$$

To calculate the control law u_{sd} and u_{sq} of the complete system [20], we define the second step, two new errors are defined for the components of the stator current given by:

$$\begin{cases} e_{i_{sd}} = i_{sdref} - i_{sd} \\ e_{i_{sq}} = i_{sqref}^* - i_{sq} \end{cases} \quad (14)$$

By replacing equation (12) into equation (14) we obtain:

$$\begin{cases} e_{i_{sd}} = \dfrac{T_r}{M_{sr}} \left(K_\varphi e_\varphi + \dot{\varphi}_{ref} + \dfrac{\varphi_{rd}}{T_r} \right) - i_{sd} \\ e_{i_{sq}} = \dfrac{1}{\eta \varphi_{rd}} \left(\dot{\omega}_{ref} + K_\omega e_\omega + \dfrac{F.\omega}{J} + \dfrac{T_L}{J} \right) - i_{sq} \end{cases} \quad (15)$$

New Lyapunov function based on the errors of speed, rotor flux and of the stator currents, which is given by the following expression:

$$V_2 = \frac{1}{2} \left(e_\Psi^2 + e_\omega^2 + e_{i_{sd}}^2 + e_{i_{sq}}^2 \right) \quad (16)$$

The derivative of V_2 can be written as:

$$\dot{V_2} = \left(-k_\varphi e_\varphi^2 - k_\omega e_\omega^2 - k_{i_{sd}} . e_{i_{sd}}^2 - k_{i_{sq}} . e_{i_{sq}}^2\right) + e_{i_{sq}} \left(k_{i_{sq}} . e_{i_{sq}} + \dot{i_{sq}} - \delta_1 - \frac{1}{\sigma L_s} u_{sq} + \eta \varphi_{rd} e_\omega \right) \quad (17)$$

$$+ e_{i_{sd}} \left(k_{i_{sd}} . e_{i_{sd}} + \dot{i_{sd}} - \delta_2 - \frac{1}{\sigma L_s} u_{sd} + \frac{M_{sr}}{T_r} e_\varphi \right)$$

With $k_{i_{sd}}$ and $k_{i_{sq}}$ are positive constant. We consider u_{sd} and u_{sq} as virtual commands of our second subsystem, and with a suitable choice of these we will render V_2 negative and stabilize the subsystem. From where we draw:

$$\begin{cases} u_{sd} = \sigma L_s \left(k_{i_{sd}} e_{i_{sd}} - \delta_1 + \dot{i}_{sdref} + \frac{M_{sr}}{T_r} e_{\varphi} \right) \\ u_{sq} = \sigma L_s \left(k_{i_{sq}} e_{i_{sq}} - \delta_2 + \dot{i}_{sqref} + \eta \varphi_{rd} e_{\omega} \right) \end{cases} \tag{18}$$

With:

$$\begin{cases} \delta_1 = -\gamma i_{sd} + n_p \omega i_{sq} + \frac{\mu}{T_r} \varphi_{rd} + \frac{M_{sr}}{T_r} \frac{i_{sq}^2}{\varphi_{rd}} \\ \delta_2 = -\gamma i_{sq} - n_p \omega i_{sd} - \mu n_p \omega \varphi_{rd} - \frac{M_{sr}}{T_r} \frac{i_{sd} i_{sq}}{\varphi_{rd}} \end{cases} \tag{19}$$

Where:

$$\gamma = \frac{M_{sr}^2 R_r + R_s L_r^2}{\sigma L_s L_r^2}, \eta = \frac{n_p M_{sr}}{J L_r}, \mu = \frac{M_{sr}}{\sigma L_s L_r}, T_r = \frac{L_r}{R_r}$$

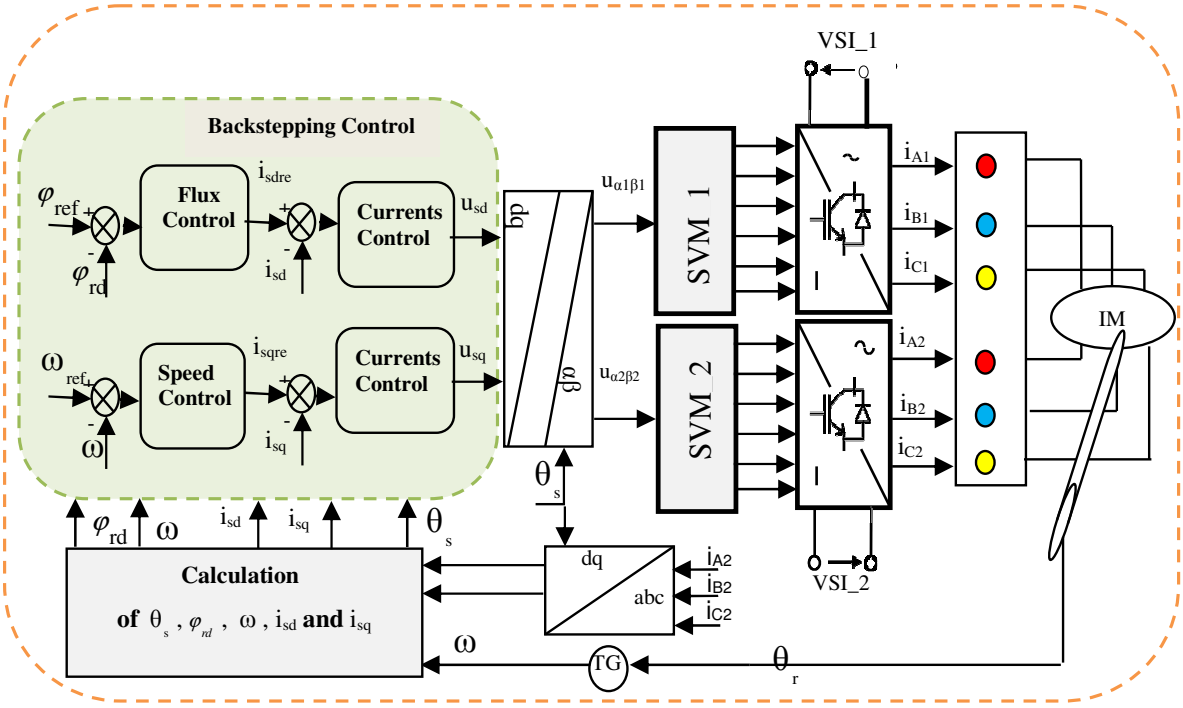

Figure 6 The schematic diagram of backstepping control using space vector modulation.

Therefore, the derivative of V_2 becomes such as:

$$\dot{V}_2 = \left(-K_{\varphi} e_{\varphi}^2 - K_{\omega} e_{\omega}^2 - K_{isd} e_{isd}^2 - K_{isq} e_{isq}^2 \right) \prec 0 \tag{20}$$

Finally, the block diagram of control by backstepping using space vector modulation of open-end winding induction motor taking account the stator faults is presented in Figure.6.

3. SIMULATION RESULTS

The block diagram of Backstepping control based on SVM of IM with open-end stator winding is shown in Figure. 6. The proposed control is carried out through MATLAB

simulations. The parameters of the motor used for modeling studies are listed as follows: $n_p = 2$: Number of pole pairs, $R_s = 1.63\Omega$: Stator resistance, $L_s = 142mH$: Stator cyclic inductance, $M_{sr} = M_{rs} = 10mH$: Mutual inductance stator-rotor, $R_r = 0.93\Omega$: Rotor resistance, $L_r = 76mH$: Rotor cyclic inductance, $J = 0.011N.m.s^2$: moment of inertia.

$N_s = 160, N_{cc} = 0 \Rightarrow 0\% \rightarrow h_{sa} = h_{sb} = h_{sc} = 1$: The coefficients in healthy mode operation

$N_s = 160, N_{cc} = 30 \Rightarrow 18.75\% \rightarrow h_{sa} = 0.8125, h_{sb} = h_{sc} = 1$
$N_s = 160, N_{cc} = 60 \Rightarrow 37.5\% \rightarrow h_{sa} = 0.625, h_{sb} = h_{sc} = 1$: The coefficients in faulty mode operation
$N_s = 160, N_{cc} = 80 \Rightarrow 50\% \rightarrow h_{sa} = 0.5, h_{sb} = h_{sc} = 1$

When a short-circuits between turns, different levels of failures are tested with, N_{cc} =30, N_{cc} =60 and N_{cc} =80 the number of turns in short-circuit and N_s=160 the number of turns in healthy regime. The simulation results have been obtained with no load as starting up condition and the load is changed to 2 N.m at t=2 s, with the rated speed to 300 rad/sec. The waveforms of the rotor speed, the electromagnetic torque, the amplitude of rotor flux and the stator currents at various load and fault conditions obtained from simulation are presented in Figure. 7 to 10.

Figure 7 to 9 show respectively the simulation result of the rotor speed, the electromagnetic torque and the rotor flux amplitude and its zooms with; Zoom A shows N_{cc}=0 equivalent 0% at 0s to 3s, Zoom B= shows N_{cc}=30 equivalent 18.75% at 3s, Zoom C shows N_{cc}=60 equivalent 37.5% at 4s and Zoom D shows N_{cc}=80 equivalent 50 % at 5s of the healthy motor and the different types of short-circuits between turns. From this waveforms, we notice that the waveforms has a little oscillations which can be ignored for low numbers of 18.75% and 37.5% turns in short-circuit, and increases the oscillations in the case of a short-circuit which touch 50% of the turns. This oscillations is related to the number of coils in short-circuit. We also noticed the rotor speed is very close to the reference and faster dynamic response of torque. We record, from the waveform of three phase stator current (see Figure.10), it can be observed that the stator currents after the appearance of default, increases in the phase affected compared to the regime healthy. This is obviously the simultaneous decrease of stator resistance.

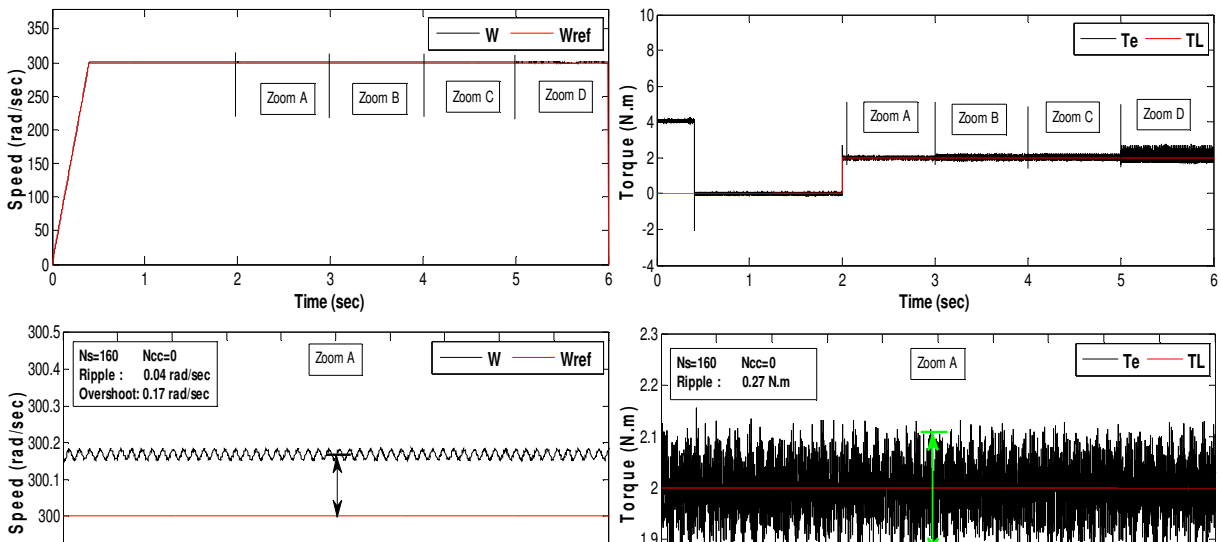

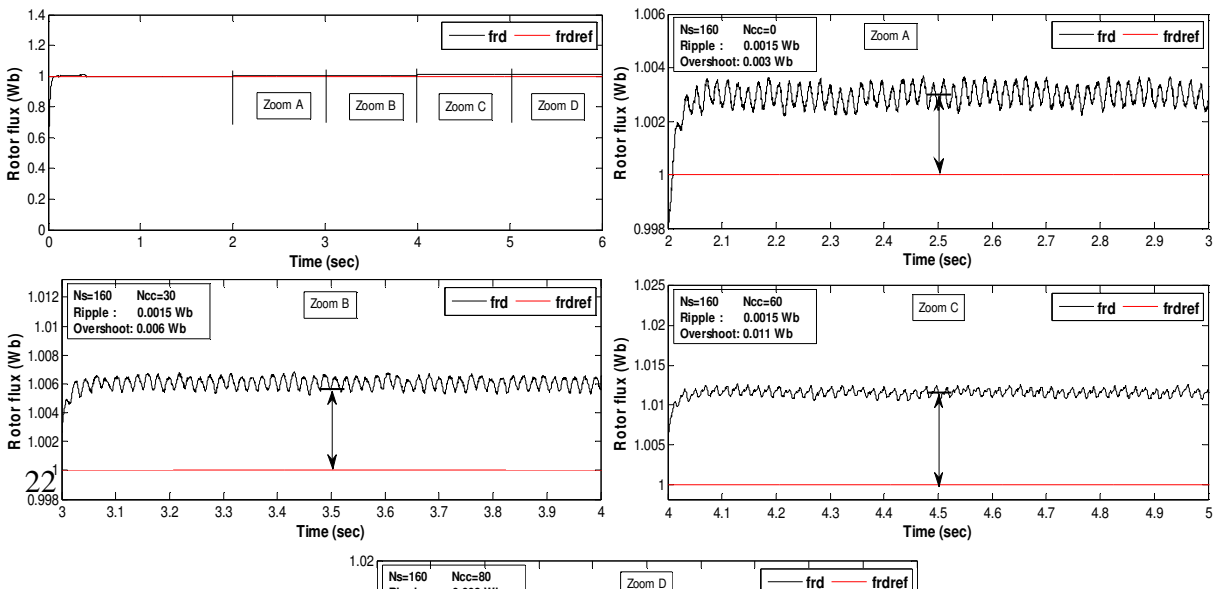
frd
frdref
Zoom A
Zoom B
Zoom C
Zoom D
Rotor flux (Wb)
Time (sec)
Ns=160 Ncc=0
Ripple : 0.0015 Wb
Overshoot: 0.003 Wb
Ns=160 Ncc=30
Ripple : 0.0015 Wb
Overshoot: 0.006 Wb
Ns=160 Ncc=60
Ripple : 0.0015 Wb
Overshoot: 0.011 Wb
Ns=160 Ncc=80

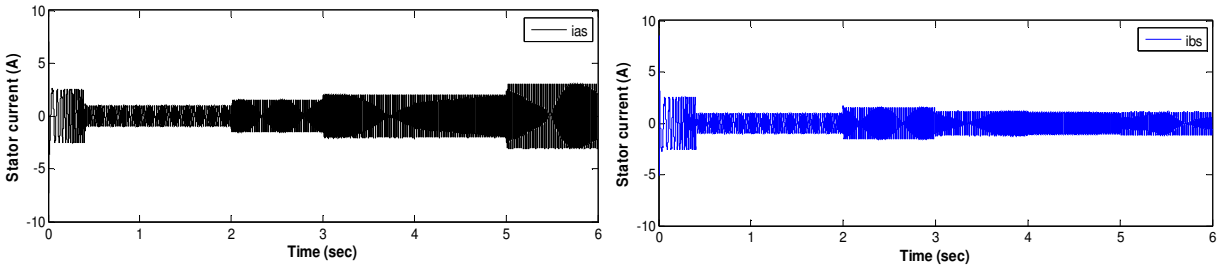

Figure 10 The wave of stator currents

Table 1 summarizes the different levels of failures are tested, when the motor was running with load is changed to 2 N.m at t=2 s.

		N_s=160			
Performance		N_{cc}=0	N_{cc}=30	N_{cc}=60	N_{cc}=80
W (rad/s)	Ripple (rad/s)	0.04	0.05	0.06	0.16
	Overshoot (rad/s)	0.17	0.17	0.18	0.13
Ψ_r (Wb)	Ripple (Wb)	1.5e-3	1.5e-3	1.5e-3	3e-3
	Overshoot (Wb)	0.003	0.006	0.011	0.01
T_e (N.m)	Ripple (N.m)	0.27	0.37	0.48	1
ZOOM		**Zoom A**	**Zoom B**	**Zoom C**	**Zoom D**

Table 1 A comparative study between backstepping-SVM control under the healthy and faulty conditions.

From Figure. 7 to 10, and the Table 1, the proposed Backstepping-SVM strategy has the ability to rejection the effect of these faults and it ensures convergence of the different levels of a short-circuits between turns.

4. CONCLUSIONS

The objective of this work is the study of the problems that can affect the operation of open-end winding induction motor through failures, especially short-circuit faults between turns, to its impact on the control and operation of the machine. In addition, a backstepping control based on space vector modulation is used to ensure the continuous operation of the

motor before the required maintenance can be done. The obtained results confirm that the proposed Backstepping-SVM strategy has the ability of rejecting the effect of stator faults. This is an interesting characteristic in favour of the industrial applications where the highest reliability must be preserved. Also this will allow us to avoid frequent stops of industrial processes.

REFERENCES

[1] W. Yang, D. Panda, T. A. Lipo and P. Di, "Open-winding power conversion systems fed by half-controlled converters," IEEE Trans. on Power Electronics, Vol. 28, No. 5, pp. 2427-2436, May. 2013.

[2] W.T. Thomson and M. Fenger, "Current Signature Analysis to Detect Induction Motor Faults," IEEE industry Applications Magazine, Vol. 7, No. 4, pp. 26-34, Jul/Aug. 2001.

[3] G. Bossio, C.D. Angelo, J. Solsona, G. García and M. I. Valla, "A 2-D Model of the Induction Machine: Extension of the Modified Winding Function Approach," IEEE Trans. on Energy Convertion, Vol. 19, No. 1, pp. 144-150, March. 2004.

[4] G. M. Joksimovic, and J. Penman, "The Detection of Inter-Turn Short Circuits in the Stator Windings of Operating Motors," IEEE Trans. on Industrial Electronics, Vol. 47, No. 5, pp. 1078-1084, Oct. 2000.

[5] G. Amal, B. Hanen, P. Remus, S. Anis, R. Raphael and M.· Mohamed, "Detecting Inter-Turn Short-Circuit Fault in Induction Machine Using High-Order Sliding Mode Observer: Simulation and Experimental Verification," Journal of Control, Automation and Electrical Systems, Vol. 28, No. 4, pp. 532-540, August. 2017.

[6] A. Siddique, G. S. Yadava and B. Singh, "A review of stator fault monitoring techniques of induction motors," IEEE Trans. on Energy Conversion, Vol. 20, No. 1, March. 2005.

[7] A. Bellini, F. Filippetti, C. Tassoni and G. A. Capolino, "Advances in diagnostic techniques for induction machines", IEEE Trans. on Industrial Electronics, Vol.55, No. 12, Dec. 2008.

[8] F. Ying, Z. Weixia, Z. Xiangyang and Z. Li, "Stator Winding Inter-turn Short Circuit Faults Severity Detection Controlled by OW-SVPWM without CMV of Five-phase FTFSCW-IPM," 18th International Conference on Electrical Machines and Systems (ICEMS) of IEEE, Pattaya City, Thailand, pp. 1192-1197, Oct. 2015.

[9] M. Sahraoui, A. Ghoggal, S. E. Zouzou A. Aboubou and H. Razik, " Modelling and Detection of Inter-Turn Short Circuits in Stator Windings of Induction Motor," 32nd Annual Conference on IEEE Industrial Electronics, Paris, France, pp. 4981-4986, Nov. 2006.

[10] J. Penman, H. G. Sedding, B. A. Lloyd and W. T. Fink, "Detection and Location of Inter-Turn Short Circuits in the Stator Windings of Operating Motors", IEEE Trans. on Energy Conversion, Vol. 9, No.4, pp. 652-658, Dec. 1994.

[11] E. Schaeffer, "Diagnostic des machines asynchrones: modèle et outils paramétriques dédiés à la simulation et à la détection des défauts", Thèse de Doctorat, Ecole générale de Nantes, France, 1999.

[12] T. Boumegoura, "Recherche de signature électromagnétique des défauts dans une machine asynchrone et synthèse d'observateurs en vue du diagnostic", Thèse de doctorat, L'école Doctorale Electronique, Electrotechnique, Lyon, 2001.

[13] Y. Amara and G. Barakat, "Modeling and Diagnostic of Stator Faults in Induction Machines Using Permeance Network Method", PIERS Proc, Marrakesh, MOROCCO, pp. 1550-1558, March. 2011.

[14] H. Nguyen, S. Jeevanand and D. Wang, "Model-Based Diagnosis and RUL Estimation of Induction Machines under Inter-Turn Fault," IEEE Trans. on Industry Applications, Vol. 99, pp. 19-31, Feb. 2017.

[15] H. A. Toliyat and T. A. Lipo, "Transient analysis of cage induction machines under stator, rotor bar and end ring faults," IEEE Trans. on Energy Conversion, Vol. 10, No. 2, pp. 241-247, June 1995.

[16] A. I. Megahed and O. P. Malik, "Synchronous generator internal fault computation and experimental verification," Proc. IEE-Generation, Transmission, Distrib, Vol. 145, No. 5, pp. 604-610, Sept. 1998.

[17] V. A. Kinitsky, "Digital computer calculation of internal fault currents in a synchronous machine," IEEE Trans. on Power Apparatus and Systems, Vol. 87, No. 8, pp. 1675–1679, Aug. 1968.

[18] A. Lebaroud and G. Clerc, "Analysis of stator short-circuit faults for induction machine using finite element modeling", 7th International Multi- Conference on Systems, Signals and Devices of IEEE, Amman, Jordan. June. 2010.

[19] K. Djalal Eddine and K. Aissa, " Three-phases Model of the Induction Machine Taking Account the Stator Faults", International Journal of Mechanical and Mechatronics Engineering, Vol. 3, No. 4, pp. 363-366, 2009.

[20] B. Ali, M. Abdellah and T. Rachid , "Backstepping Control of Induction Motor Fed by Five-Level NPC Inverter,"(IJACSA) International Journal of Advanced Computer Science and Applications, Vol. 7, No. 10, Oct. 2016.

[21] A. Bennassar, A. Abbou, M. Akherraz and M. Barara, "Sensorless Backstepping Control Using an Adaptive Luenberger Observer with Three Levels NPC Inverter," International Journal of Computer, Electrical, Automation, Control and Information Engineering, Vol. 7, No. 8, January. 2013.

[22] A. Tarek, M. Arezki, T. Hicham, H. Imadeddine and A. Abdelkarim, "Backstepping Control for Induction Motor Drive Using Reduced Model in Healthy State: Simulation and Experimental Study," Proc. 6th International Conference on Systems and Control of IEEE, Batna, Algeria, May. 2017.